Available online at www.sciencedirect.com

SciVerse ScienceDirect

Journal of the European Ceramic Society 32 (2012) 291–298

www.elsevier.com/locate/jeurceramsoc

Effect of K_2O on structure–property relationships and phase transformations in Li_2O–SiO_2 glasses

Hugo R. Fernandes [a,*], Dilshat U. Tulyaganov [a,b], Ashutosh Goel [c], José M.F. Ferreira [a]

[a] Department of Ceramics and Glass Engineering, University of Aveiro, CICECO, 3810-193 Aveiro, Portugal
[b] Turin Polytechnic University in Tashkent, 17, Niyazova str., 100174 Tashkent, Uzbekistan
[c] Glass Processing Group, Radiological and Nuclear Science and Technology Division, Pacific Northwest National Laboratory, Richland, WA 99354, United States

Received 3 August 2011; accepted 18 September 2011
Available online 8 October 2011

Abstract

Glass compositions with formula $(71.78 - x)SiO_2$–$2.63Al_2O_3$–$(2.63 + x)K_2O$–$23.7Li_2O$ (mol.%, $x = 0$–10) and SiO_2/Li_2O molar ratios far beyond that of stoichiometric lithium disilicate ($Li_2Si_2O_5$) were prepared by conventional melt-quenching technique to investigate the influence of K_2O content on structural transformations and devitrification behaviour of glasses in the Li_2O–SiO_2 system. The scanning electron microscopy (SEM) examination of as cast non-annealed glasses revealed the presence of nanosized droplets in glassy matrices suggesting occurrence of liquid–liquid phase separation. An overall trend towards depolymerization of the silicate glass network with increasing K_2O content was demonstrated by employing magic angle spinning-nuclear magnetic resonance (MAS-NMR) spectroscopy. The distribution of structural units in the experimental glasses was estimated using ^{29}Si MAS-NMR spectroscopy suggesting the appearance of Q^2, enhancement of Q^3 and diminishing of Q^4 groups with increasing K_2O contents. X-ray diffraction (XRD) and differential thermal analysis (DTA) were used to assess the influence of K_2O on devitrification process and formation of lithium disilicate ($Li_2Si_2O_5$) and/or lithium metasilicate (Li_2SiO_3) crystalline phases.
© 2011 Elsevier Ltd. All rights reserved.

Keywords: Glass; Glass ceramics; Lithium disilicate; Thermo-physical properties

1. Introduction

The immiscible region between the Li_2O–$2SiO_2$ and SiO_2 end members is an important feature in the Li_2O–SiO_2 system. The synthesis of glass-ceramic (GC) materials in the Li_2O–SiO_2 system is based on controlled nucleation and crystallization of lithium metasilicate and/or lithium disilicate phases which govern the properties for the final product. The glasses with SiO_2 contents higher than the stoichiometric $Li_2O{\cdot}2SiO_2$ (33.33 mol.% Li_2O–66.66 mol.% SiO_2) tend to separate into a matrix phase with a composition almost similar to that of lithium disilicate along with an isolated droplet SiO_2 rich phase,[1] while glasses with Li_2O contents <30 mol.% usually turn out to be opalescent or opaque on cooling owing to phase separation.[1–3] Although, nucleation of base glass with stoichiometric composition of lithium disilicate has been widely investigated for GC manufacture,[4] the GCs derived from this parent binary system exhibit some unfavourable characteristics in terms of their mechanical and chemical properties which hinder their potential applications in several technological areas.

On the other hand, lithium disilicate GCs derived from non-stoichiometric compositions have proven themselves to be potential candidates for different functional applications, for example: dental restorations,[5–8] metal-glass seals,[9,10] etc. Fundamental research on certain non-stoichiometric lithium disilicate based glass compositions was carried out by Stookey (1959).[11] It is noteworthy that according to Höland and Beal,[4] the term 'non-stoichiometric' implies that SiO_2/Li_2O molar ratio deviates greatly from 2:1 and the system in rendered considerably more complex with numerous additional components and nucleating agents. However, the present investigation aims towards investigating a relatively simpler non-stoichiometric lithium disilicate based GC system in the glass forming region of Li_2O–K_2O–Al_2O_3–SiO_2 with its SiO_2/Li_2O molar ratio varying between 2.69 and 3.13. The simultaneous incorporating of K_2O and Al_2O_3 is known to significantly improve the chemical

* Corresponding author.
E-mail address: h.r.fernandes@ua.pt (H.R. Fernandes).

0955-2219/$ – see front matter © 2011 Elsevier Ltd. All rights reserved.
doi:10.1016/j.jeurceramsoc.2011.09.017

Table 1
Compositions of the experimental glasses.

	Oxides (mol.%)				SiO_2/Li_2O	SiO_2/K_2O	K_2O/Al_2O_3
	Li_2O	K_2O	Al_2O_3	SiO_2			
GK_0	22.96	2.63	2.63	71.78	3.13	27.29	1.00
$GK_{0.5}$	22.96	3.13	2.63	71.28	3.10	22.77	1.19
GK_1	22.96	3.63	2.63	70.78	3.08	19.50	1.38
$GK_{1.5}$	22.96	4.13	2.63	70.28	3.06	17.02	1.57
GK_2	22.96	4.63	2.63	69.78	3.04	15.07	1.76
$GK_{2.5}$	22.96	5.13	2.63	69.28	3.02	13.50	1.95
GK_5	22.96	7.63	2.63	66.78	2.91	8.75	2.90
GK_{10}	22.96	12.63	2.63	61.78	2.69	4.89	4.80

durability of lithium disilicate GCs,[1,12,13] therefore justifying the choice of these two oxides in the present study. One of the main objectives of this study was to investigate the influence of replacing increasing amounts of SiO_2 by equimolar amounts of K_2O on the structural transformations occurring in the non-stoichiometric lithium disilicate glasses, and on their crystallization mechanism.

2. Experimental procedure

2.1. Glass preparation

The investigated glass compositions were designed according to the general formula $(71.78 - x)$ SiO_2–$2.63Al_2O_3$–$(2.63 + x)$ K_2O–$23.7Li_2O$ (mol.%), where x changed from 0 to 10, with SiO_2/Li_2O ratios far from lithium disilicate stoichiometry ($SiO_2/Li_2O = 2$). Accordingly, the glasses have been labelled as GK_x depending on the amount of K_2O being substituted for SiO_2 in the glass compositions. For example: GK_0 corresponds to the parent composition, i.e. $x = 0$ and $K_2O/Al_2O_3 = 1$. Table 1 presents the detailed composition of the glasses along with their corresponding SiO_2/Li_2O, SiO_2/K_2O and K_2O/Al_2O_3 ratios.

A total of eight glasses were prepared in Pt-crucibles using melt quenching technique. The powders of technical grade SiO_2 (purity >99.5%) and of reactive grade Al_2O_3, Li_2CO_3, and K_2CO_3 were used. Homogeneous mixtures of batches (~100 g), obtained by ball milling, were calcined at 800 °C for 1 h and then melted in Pt crucibles at 1550 °C for 1 h, in air. The glasses were produced in bulk (monolithic) form by pouring glass melts on bronze mould in two different sets. The glasses of one set were immediately annealed at 450 °C for 1 h; the other set of glasses was preserved in the non-annealed condition.

2.2. Thermo-physical properties of glasses

The coefficient of thermal expansion (CTE) of the annealed glasses was measured by dilatometry using prismatic samples of bulk glasses with cross section of $3 \times 4\ mm^2$ (Bahr Thermo Analyse DIL 801 L, Germany; heating rate $5\ K\ min^{-1}$). The differential thermal analysis (DTA, Setaram Labsys, Setaram Instrumentation, Caluire, France) of glasses was carried out in air from room temperature to 1000 °C at heating rate (β) of $20\ K\ min^{-1}$. The glass powders with sizes in the range of 500–1000 μm (collected by sieving of crushed non-annealed glass blocks) and weighing 50 mg were contained in an alumina crucible and the reference material was α-alumina powder. The value of the glass transition temperature T_g, crystallization onset temperature, T_c and peak temperature of crystallization, T_p were obtained from the DTA scans.

Archimedes' method (i.e. immersion in ethylene glycol) was employed to measure the apparent density of the bulk annealed glasses which was further applied along with compositions of glasses to calculate their excess volume (V_e) according to a procedure described elsewhere.[3]

2.3. Structural characterization of glasses

^{29}Si MAS-NMR spectra were recorded on a Bruker ASX 400 spectrometer operating at 79.52 MHz (9.4 T) using a 7 mm probe at a spinning rate of 5 kHz. The pulse length was 2 μs and 60 s delay time was used. Kaolinite was used as the chemical shift reference. ^{27}Al MAS-NMR spectra were recorded on a Bruker ASX 400 spectrometer operating at 104.28 MHz (9.4 T) using a 4 mm probe at a spinning rate of 15 kHz. The pulse length was 0.6 μs and 4 s delay time was used. $Al(NO_3)_3$ was used as the chemical shift reference. The Q^n distributions were obtained by curve fitting and spectral deconvolution using DMFIT program (version 2011).[14]

2.4. Crystalline phase analysis and microstructural evolution in glass-ceramics

Bulk parallelepiped glass samples were heat treated non-isothermaly at 600, 700, 800 and 900 °C for 1 h, respectively, at a heating rate of $2\ K\ min^{-1}$. The amorphous nature of the parent glasses and the nature of crystalline phases present in the GCs were determined by X-ray diffraction (XRD) analysis (Rigaku Geigerflex D/Mac, C Series, Japan; Cu Kα radiation, 2θ between 10° and 60° with a 2θ-step of $0.02\ ^\circ\ s^{-1}$). The crystalline phases were identified by comparing the obtained diffractograms with patterns of standards complied by the International Centre for Diffraction Data (ICDD).

Microstructure observations were done at polished (mirror finishing) and then etched surfaces of samples (by immersion in 2 vol.% HF solution for 1–2 min) by field emission

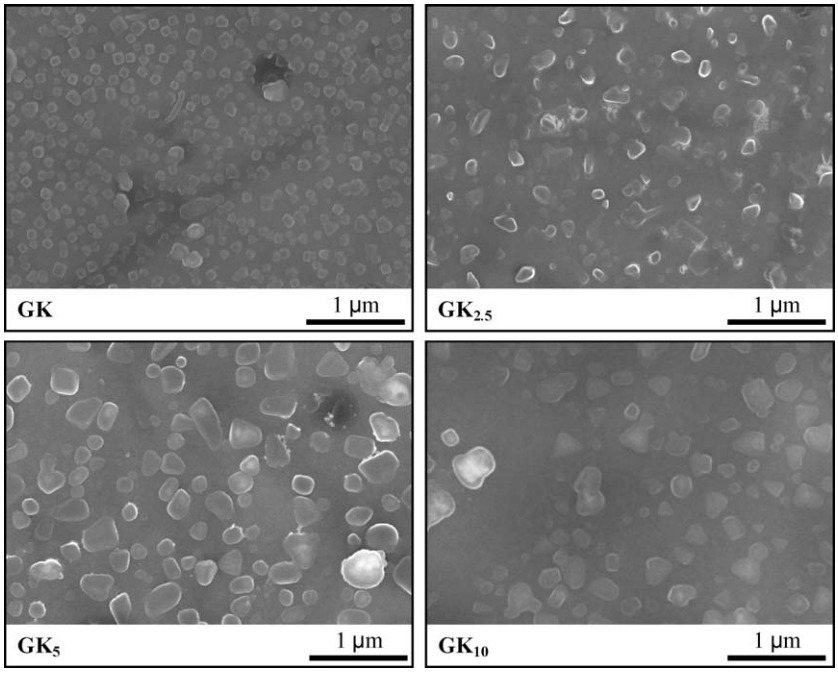

Fig. 1. SEM images of the experimental non-annealed bulk glasses (etched with 2 vol.% HF solution for 1 min).

scanning electron microscopy (SEM, Hitachi SU-70, Japan) under secondary electron mode.

3. Results and discussion

3.1. Casting ability and microstructure of glasses

Heating at 1550 °C for 1 h was adequate to obtain bubble-free, homogenous transparent and colourless glasses from all the investigated compositions. The absence of any crystalline inclusions was confirmed by XRD and SEM analyses. The SEM images of as cast non–annealed samples (Fig. 1) revealed nanosized droplets embedded in the glass matrices of all investigated compositions suggesting the occurrence of liquid–liquid phase separation. The droplet size and density distribution observed in the phase separated zones were small enough to avoid Tyndall effect, thus, resulting in transparent glasses. It is noteworthy that liquid separation is often the precursor to nucleation and crystal growth in certain GC compositions and can profoundly influence the crystallization path.[1,15] According to Vogel,[1] metastable immiscibility that occurs in binary Li_2O–SiO_2 system causes segregation of glassy phase into droplet-like zones of Li-rich phase and SiO_2-rich glass matrix. Moreover, the mean droplet size was found to be a function of Li_2O and SiO_2 contents. In particular, a bell-shaped curve showed maxima for $SiO_2/Li_2O = 4.95$ (~16.8 mol.% of Li_2O) and minima for both pure silica glass and stoichiometric lithium disilicate composition. Assuming similar structural roles for Li_2O and K_2O in the investigated glasses, a steady decrease in size of droplet-like zones should be expected with increasing contents of K_2O. However, our experimental results presented in Fig. 1 show an opposite trend with the mean droplet size growing with increasing K_2O contents. This can be explained by the preferential distribution of K_2O in the Li_2O-rich droplets[15] preventing diffusion of Li_2O towards SiO_2 rich region. Consequently, a composition gradient between separated droplet-like zones and silica rich glassy matrix becomes greater with increasing content K_2O leading to less homogeneous glass structures. The gradual lowering of SiO_2 content in glasses and the consequentially decrease in volume fraction of the silica-rich phase is expected to enhance the droplet like Li_2O and K_2O rich phase.[16]

3.2. Structure-property relationships in glasses

3.2.1. Density, V_e, CTE and T_g

The density values of annealed glasses varied in the range of 2.36–2.43 g cm^{-3} (Table 2). A slight increase in density was observed from the parent glass composition (GK_0) to the glass $GK_{0.5}$, followed by a broad plateau until glass GK_2, and a new step increment to the glass $GK_{2.5}$. After that, density increased in direct proportion with further added amount of K_2O reaching the highest value for the glass GK_{10}. Since, density of glasses is an additive property, therefore, the constant values of glass density for compositions $GK_{0.5}$, GK_1, $GK_{1.5}$ and GK_2 may be attributed to the small K_2O increments in the glasses. However, sound conclusions regarding the structure of glasses cannot be drawn merely on the basis of density variations.[17] Therefore, in order to obtain a clear trend about the influence of K_2O/SiO_2 ratio on structure of investigated glasses, the values of excess molar volume (V_e) were calculated from density and glasses' molar composition data and featured a decrease of excess volume of glasses with increasing x values (Table 2). The incorporation of the K_2O network modifier alters the glass properties. The formation of less directed ionic bonds makes the structural skeleton to collapse into a closer packing, thus leading to reduced degree of cross-linking, which, in turn, reduces the glass transition

Table 2
Thermo-physical properties of the experimental glasses.

	d (g cm^{-3})	V_e (cm^3 mol^{-1})	NBO/T	CTE ± 0.1 (10^{-6} K^{-1})	T_g ± 2 (°C)	T_c ± 2 (°C)	T_p ± 2 (°C)
GK_0	2.36 ± 0.01	1.26 ± 0.01	0.60	9.65	505	702	821
$GK_{0.5}$	2.37 ± 0.01	1.12 ± 0.04	0.61	10.16	504	698	817
GK_1	2.37 ± 0.01	1.08 ± 0.05	0.63	11.52	503	695	806
$GK_{1.5}$	2.37 ± 0.01	1.11 ± 0.04	0.65	11.34	501	663	818
GK_2	2.37 ± 0.01	1.03 ± 0.01	0.67	11.41	502	667	812
$GK_{2.5}$	2.38 ± 0.01	0.97 ± 0.01	0.68	11.51	500	663	800
GK_5	2.40 ± 0.01	0.76 ± 0.01	0.78	12.70	496	658	778
GK_{10}	2.43 ± 0.01	0.34 ± 0.02	0.98	14.68	481	582	723

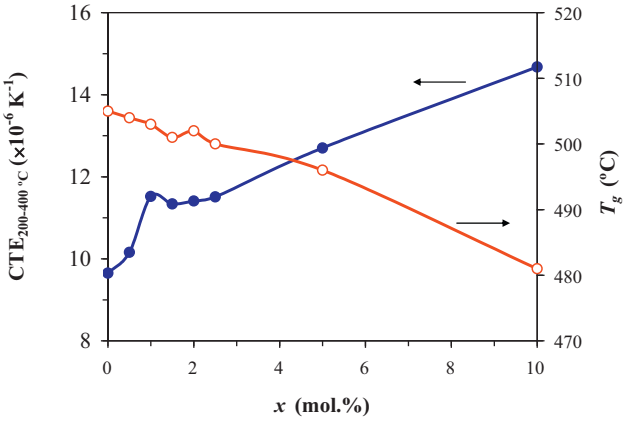

Fig. 2. Evolution of CTE and T_g with the amount of K_2O added to the parent composition.

temperature (T_g) (Fig. 2). Further, an increased polarizability arising from the negatively charged non-bridging atoms enhances the anharmonicity of thermal vibrations, thus leading to an increase in the CTE of glasses (Table 2; Fig. 2).[18]

Furthermore, the kinks observed in the values of CTE and T_g (Fig. 2) as well as in the values of V_e (Table 2), when x ranged from 0.5–1.5, can be attributed to the progressive changes brought by the network modifier, thus making the function of less basic so-called intermediate oxides somewhat ambiguous. In the present system, below a certain Li_2O/K_2O ratio, further adding the basic modifier oxide (i.e. K_2O) into the glasses forces Li_2O to enter the glass network. This gives rise to the formation of $(LiO_{4/2})^{3-}$ structural units with a coordination number of 4. Therefore, strengthening the silicate glass network occurs.[18]

3.2.2. MAS-NMR

The ^{29}Si MAS-NMR spectra of glasses GK_0, GK_5 and GK_{10} are plotted in Fig. 3 while chemical shifts (δ), linewidths ($\Delta\delta$) and area fractions (%) of the signal components are presented in Table 3. In general, the spectra feature broad bands, which indicate the amorphous nature of these materials. For each composition, a resonance line covers the chemical shift range of silicon in several Q^n groups with $n = 0, \ldots, 4$.[19] In particular, the ^{29}Si MAS-NMR spectra for parent glass composition GK_0 is centred at about −94 ppm (Fig. 3), suggesting a mixture of Q^3 and Q^4 (Table 3). An overall trend towards depolymerization of the silicate glass network with increasing K_2O content can be observed due to the following factors: (a) centering of ^{29}Si MAS-NMR spectra at lower values, (b) formation of Q^2 groups, (c) increasing Q^3 and diminishing Q^4 units. However, the ^{29}Si spectrum for glass GK_1 (not shown) deviates from that trend, exhibiting a chemical shift centred at about −95 ppm, thus implying towards an increasing polymerization, the reasoning for this was explained in the previous section. Schramm et al.[20] investigated the extent of Q^n distributions for lithium silicate glasses in the composition region between 15 and 40 mol.% Li_2O by ^{29}Si MAS NMR spectroscopy. Values for the mean chemical shifts used to fit the spectra of those glasses were −107 ppm (Q^4), −92 ppm (Q^3), −82 ppm (Q^2), −69 ppm (Q^1), and −63 ppm (Q^0). The three major species Q^4, Q^3, and Q^2 were revealed. The percentage of Q^4 decreases with increasing Li_2O content, that of Q^3 goes through a maximum at 30 mol % Li_2O, and the percentage of Q^2 showed tendency to grow at higher Li_2O concentrations. Particular emphasis should be addressed to $22.5Li_2O$–$77.5SiO_2$ and $24Li_2O$–$76SiO_2$ glasses owing to their Li_2O content and SiO_2/Li_2O ratios comparable with the compositions investigated in our work. According to Schramm et al.[20] the $22.5Li_2O$–$77.5SiO_2$ glass composition featured the distribution of Q^n groups such as 0.1% $Q^0 + Q^1$, 3.9% Q^2, 63.2% Q^3, 32.8% Q^4 while the $24Li_2O$–$76SiO_2$ glass composition presented the following distribution: 2.5% $Q^0 + Q^1$, 11.1% Q^2, 56.6% Q^3, 29.8% Q^4. On the other hand, these glasses of Li_2O–SiO_2 system exhibited opalescence characteristic owing to precipitation of a droplet-like zones of Li-rich phase in SiO_2-rich glass matrix.[2,20] Introduction of additives such as Al_2O_3 and K_2O resulted in glasses of transparent appearance in this metastable liquid immiscibility region due to the diminishing of mean droplet diameter and the packing density of droplet phase.[2,3] Moreover, both activation energy for crystallization and crystallization rate decreased. Analysis of the ^{29}Si MAS-NMR data obtained in our study revealed that the above mentioned phenomenon can be explained by diminishing of Q^2 groups after equimolar addition of Al_2O_3 and K_2O in Li_2O–SiO_2 system. Apparently, Q^2 groups are responsible for the enhanced nucleation rate. With regard to immiscibility process, Q^2 units as well as its clustering with Q^3, which is not considered by the Q^n distribution theory, would account for the metastable liquid immiscibility region, whereas Q^4 units represent the silica-rich region.[20]

^{27}Al NMR spectra of our samples (not shown) revealed chemical shifts from 52 ppm (GK_0) to 55 ppm (GK_{10}). The peaks shifting trend in the range of 52–55 ppm usually indicates an increasing predominance of tetrahedral aluminium in the glass

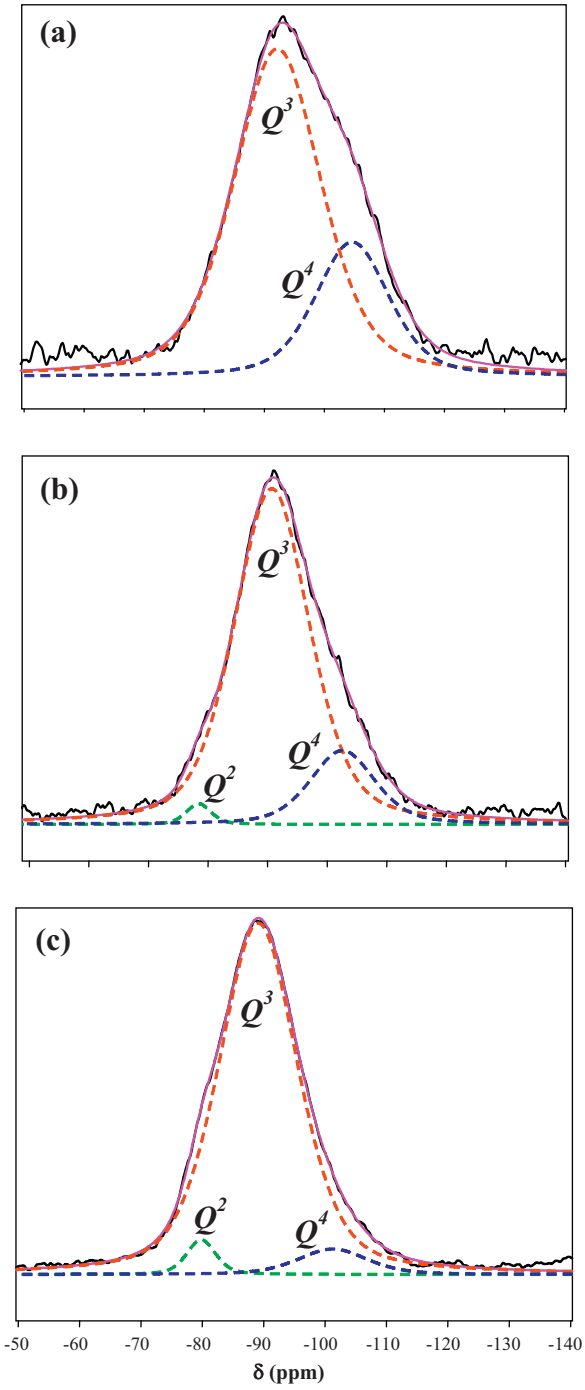

Fig. 3. ^{29}Si MAS-NMR spectra of glasses: (a) GK_0, (b) GK_5 and (c) GK_{10}. Dashed curves show the spectral deconvolution components used for fitting the data.

structure. Therefore, the results obtained suggest that the K_2O added to the parent glass tends to enhance the role of Al_2O_3 as the glass network former signifying that aluminium in a four-coordinate network-forming species would not participate in the crystallization processes. This is consistent with the need of an associated cation in the vicinity of each tetrahedral unit in order to maintain local charge neutrality of the $(AlO_{4/2})^-$ units with four bridging oxygens.[2,3] In the present case, this neutrality is assured by the presence of K_2O. In such coordination, the Al^{3+} ions strengthen the glass network and diminish crystallization tendency during melt quenching. However, as the ratio K_2O/Al_2O_3 increases, the molar concentration of K_2O exceeds that of Al_2O_3, causing the formation of a larger fraction of NBO (Table 2). These free potassium cations act as glass network modifiers and are distributed in the glass matrix apart from the glass network forming $(AlO_{4/2})^-$ units.

3.2.3. Differential thermal analysis

The DTA plots of glasses with a heating rate (β) of 20 K min^{-1}, shown in Fig. 4a, show well-defined features comprising endothermic and exothermic peaks from which transition point (T_g), temperature of onset crystallization (T_c) and peak temperature of crystallization (T_p), were determined (Table 2). In general, T_c and T_p decreased with increasing K_2O content (Fig. 4b) confirming earlier results that crystallization of K_2O containing lithium disilicate glass starts at lower temperatures.[15] Moreover, lowering of T_g values are in accordance with increasing non-bridging oxygens per tetrahedron (NBO/T) for potassium richer compositions suggesting depolymerization of glass network. Additionally it was revealed that the peak temperature of crystallization shifted to higher temperatures with increasing β (figures are not shown).

3.3. Crystallization behaviour of bulk glasses

3.3.1. Phase assemblage

Fig. 5 presents the X-ray diffractograms of glasses heat treated at different temperatures. All the investigated glass compositions were amorphous after heat treatment at 600 °C for 1 h except GK_{10} that exhibits traces of lithium metasilicate (Fig. 5a). The trend for the preferential crystallization of lithium metasilicate with increasing potassium content appears clear at 700 °C (Fig. 5b). As a matter of fact, low intensity peaks of lithium disilicate only appeared in the GK_0 sample heat treated at this temperature. Increasing the heat treatment temperature to 800 °C (Fig. 5c) favoured the formation of lithium disilicate in detriment of lithium metasilicate within the x range of 0–1, while lithium

Table 3
Solid state ^{29}Si NMR chemical shifts (δ), linewidths ($\Delta\delta$) and area fractions (%) of the signal components observed in glasses GK_0, GK_5 and GK_{10}.

x (mol.%)	Q^2			Q^3			Q^4		
	δ (ppm)	$\Delta\delta$ (ppm)	%	δ (ppm)	$\Delta\delta$ (ppm)	%	δ (ppm)	$\Delta\delta$ (ppm)	%
0	–	–	0.0	−92.2	17.2	74.3	−104.7	14.5	25.7
5	−78.4	4.9	1.7	−90.7	14.9	82.7	−102.6	12.8	15.6
10	−79.8	5.6	3.4	−89.1	15.2	90.9	−101.2	13.3	5.8

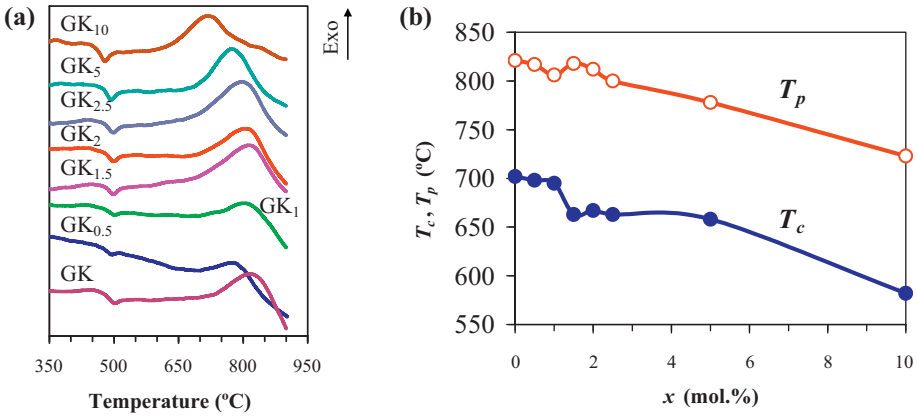

Fig. 4. Thermal behaviour of glasses: (a) DTA at $\beta = 20\,K\,min^{-1}$; (b) evolution of T_c and T_p with the amount of K_2O added to the parent composition.

metasilicate is the only phase present for $x > 1$ (also valid at 900 °C). However, the parent glass composition GK_0 underwent partial dissolution of lithium disilicate into lithium metasilicate and quartz with increasing the temperature to 900 °C, while enhanced the intensity of lithium disilicate peaks in the $GK_{0.5}$ and GK_1 compositions (Fig. 5d).

The as obtained results suggest that K_2O significantly affects the crystallization process suppressing the crystallization of lithium disilicate and promoting formation of lithium metasilicate for $x > 1$. This conclusion is in agreement with the study on equimolar replacement of 3 mol.% of Li_2O by K_2O in the $73SiO_2$, $2.15Al_2O_3$, $23.7Li_2O$ and $1.15P_2O_5$ (mol.%) base

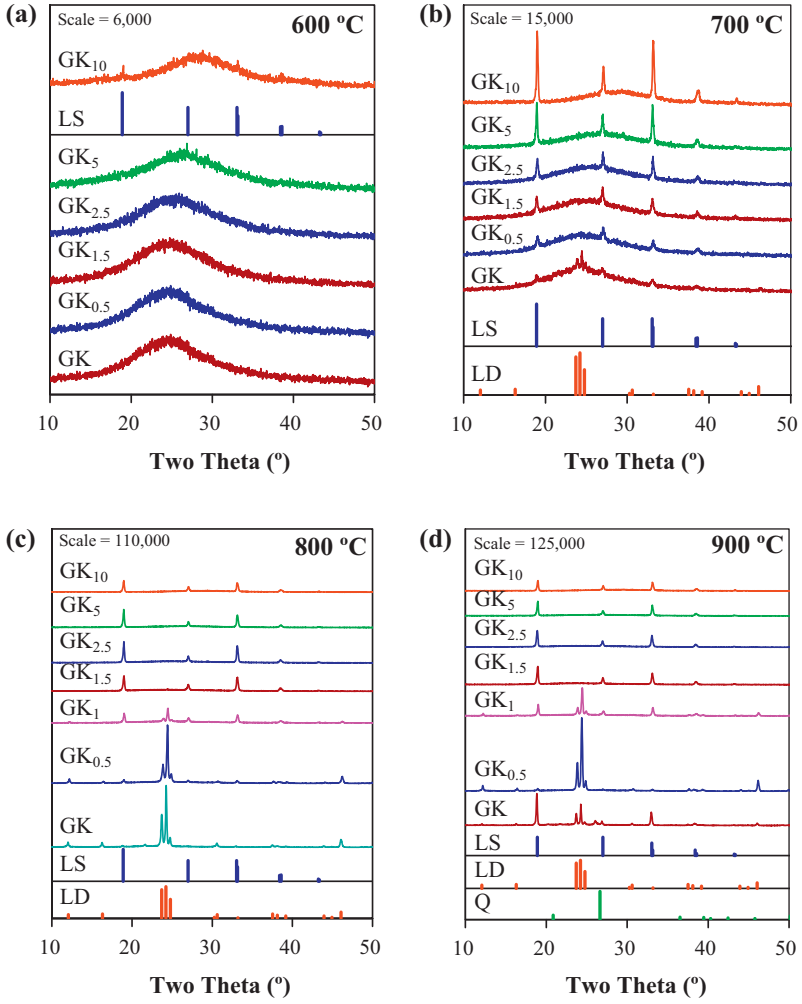

Fig. 5. X-ray diffractograms of experimental bulk glasses after heat treatment at different temperatures for 1 h. LS: lithium silicate (Li_2SiO_3, ICCD card 01-029-0828); LD: lithium disilicate ($Li_2Si_2O_5$, ICCD card 01-070-4856); Q: quartz (SiO_2, ICCD card 01-077-1060).

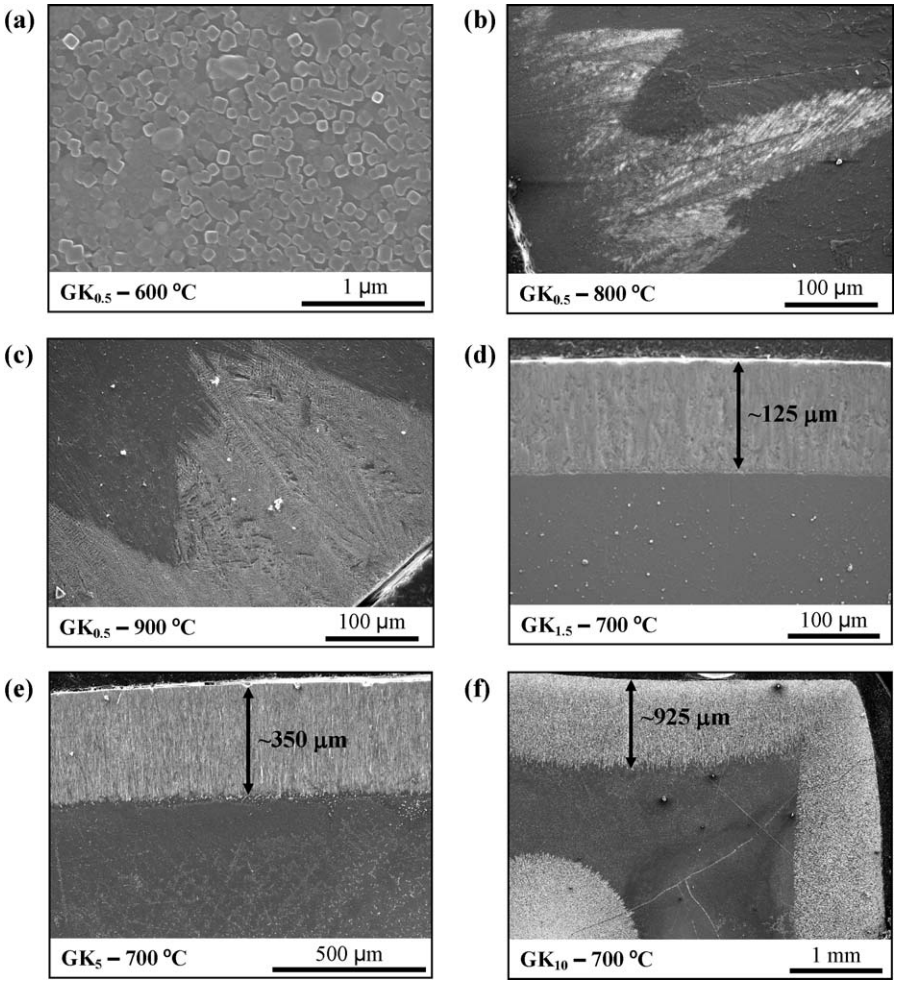

Fig. 6. SEM images of bulk glasses heat treated at different temperatures for 1 h (etched with 2 vol.% HF solution for 2 min).

glass.[15] This change in the crystallization behaviour can be explained by the lower value of the activation energy for crystallization of lithium metasilicate in comparison to that of lithium disilicate.[15,21,22] Moreover, adding alkali oxides to silicate glasses decreases the melt viscosity, increases the fraction of NBO and enhances the tendency of the glass towards devitrification.[23]

Bischoff et al. quite recently demonstrated[24] that in series with SiO_2/Li_2O molar ratio 2.39:1, at 650 °C crystalline Li_2SiO_3 is not only being formed from the Q^2 component present in the glassy precursor material but also via a disproportionation of Q^3 units in the glass according to the reaction (1):

$$2Q^3(\text{glass}) \leftrightarrow Q^2(\text{cryst.}) + Q^4(\text{glass}) \quad (1)$$

Moreover, it was revealed reveals that the Q^3/Q^4 ratio was already significantly decreased in the amorphous sample annealed at 530 °C, even before crystalline Li_2SiO_3 can be observed in either solid state NMR or X-ray powder patterns. Finally, the formation of crystalline $Li_2Si_2O_5$ in the sample annealed at 850 °C produced a strong sharp peak near −92 ppm supporting the synproportionation reaction (2):

$$Q^4(\text{glass}) + Q^2(\text{cryst.}) \leftrightarrow 2Q^3(\text{cryst.}) \quad (2)$$

Using this model and ^{29}Si MAS-NMR results (Fig. 3; Table 3) we can explain the effect of suppressing the crystallization of $Li_2Si_2O_5$ and promoting formation of Li_2SiO_3 with increasing of K_2O content. Thus, considering the significant decrease of Q^4 units in K_2O-rich glasses (e.g. GK_5 and GK_{10}) the probability of reaction (2) to occur decreases considerably. This leads to the formation of Li_2SiO_3 as a single phase directly from Q^2 or via reaction (1).

3.3.2. Microstructure

Fig. 6 shows the SEM micrographs for the glasses heat treated at different temperatures. At 600 °C, composition $GK_{0.5}$ demonstrates coalescence of droplets into bigger agglomerates (Fig. 6a). A superficial layer of crystals with dendritic morphology, characteristic for lithium metasilicate, is clearly observed in the samples heat treated at 800 °C (Fig. 6b).[3] At 900 °C, it is possible to observe the droplet-like zones of Li-rich phase, which are responsible for formation of lithium disilicate crystals in bulk region of the specimen (Fig. 6c).

The phase separation in glasses with higher K_2O contents conferred peculiar microstructural features since these glasses separate into two phases, one of which is a continuous phase rich in Li_2O and containing considerable amount of K_2O. Moreover,

the addition of K_2O seems to have favoured surface crystallization in glasses, as well as the formation of lithium metasilicate for $x > 1$, in good agreement with the XRD data. Thus, a surface layer of lithium metasilicate crystals grown towards the bulk can be clearly seen in Figs. 6d–f, for the samples heat treated at 700 °C within the x range of 1.5–10, respectively. The thickness of the crystalline surface layer increased from 125 μm ($GK_{1.5}$, Fig. 6d) to 350 μm (GK_5, Fig. 6e) and 925 μm (GK_{10}, Fig. 6f), an effect that might be due to the preferred distribution of K_2O in liquid–liquid phase separated Li_2O-rich droplets. However, further information on nucleation and crystallization mechanisms needs to be gathered via investigating the crystallization kinetics of experimental glasses.

4. Conclusions

An insight into the effect of K_2O on structure–property relationships and devitrification behaviour of glasses in the Li_2O–SiO_2 system has been presented. The results can be summarized in the following conclusions:

1. Liquid–liquid phase separation occurred in all investigated glasses and the addition of K_2O to the parent glass led to increasing the mean droplet size and their distribution density due to a decreasing energy barrier towards phase separation caused by the lowering of glass melt viscosity.
2. The ^{29}Si MAS-NMR spectra evidenced a mixture of Q^4 (Si) and Q^3 (Si) as the predominant structural units in all the glasses. Upon increasing K_2O content, new Q^2 groups appeared and the amount of Q^3 units increased, whereas the Q^4 units diminished suggesting depolymerization of the silicate glass network.
3. The ^{27}Al MAS-NMR results suggested that the K_2O added to the parent glass tends to enhance the role of Al_2O_3 as glass network former, signifying that four-coordinate aluminium network-forming species would not participate in the crystallization processes.
4. According to the ^{29}Si MAS-NMR results, diminishing of Q^4 groups in K_2O-rich glasses (e.g. GK_5 and GK_{10}) suppressed the crystallization of $Li_2Si_2O_5$ and promoted the formation of Li_2SiO_3.

Acknowledgments

Hugo R. Fernandes is grateful for the financial support of CICECO and for the PhD grant (SFRH/BD/41307/2007) from the FCT, Portugal.

References

1. Vogel W. *Structure and crystallization of glasses*. Leipzig: Pergamon Press; 1971.
2. Fernandes HR, Tulyaganov DU, Goel A, Ribeiro MJ, Pascual MJ, Ferreira JMF. Effect of Al_2O_3 and K_2O content on structure, properties and devitrification of glasses in the Li_2O–SiO_2 system. *J Eur Ceram Soc* 2010;**30**:2017–30.
3. Fernandes HR, Tulyaganov DU, Goel IK, Ferreira JMF. Crystallization process and some properties of Li_2O–SiO_2 glass-ceramics doped with Al_2O_3 and K_2O. *J Am Ceram Soc* 2008;**91**:3698–703.
4. Höland W, Beall G. *Glass-ceramic technology*. Westerville: The American Ceramic Society; 2002.
5. Borom MP, Turkalo AM, Doremus RH. Strength and microstructure in lithium disilicate glass-ceramics. *J Am Ceram Soc* 1975;**58**:385–91.
6. Guazzato M, Albakry M, Ringer SP, Swain MV. Strength, fracture toughness and microstructure of a selection of all-ceramic materials. Part I. Pressable and alumina glass-infiltrated ceramics. *Dent Mater* 2004;**20**:441–8.
7. Holand W, Apel E, van 't Hoen C, Rheinberger V. Studies of crystal phase formations in high-strength lithium disilicate glass-ceramics. *J Non-Cryst Solids* 2006;**352**:4041–50.
8. Iqbal Y, Lee WE, Holland D, James PF. Metastable phase formation in the early stage crystallisation of lithium disilicate glass. *J Non-Cryst Solids* 1998;**224**:1–16.
9. Bengisu M, Brow RK, White JE. Interfacial reactions between lithium silicate glass-ceramics and Ni-based superalloys and the effect of heat treatment at elevated temperatures. *J Mater Sci* 2004;**39**:605–18.
10. Goswami M, Kothiyal GP, Montagne L, Delevoye L. MAS-NMR study of lithium zinc silicate glasses and glass-ceramics with various ZnO content. *J Solid State Chem* 2008;**181**:269–75.
11. Stookey SD. Catalyzed crystallization of glass in theory and practice. *Ind Eng Chem* 1959;**51**:805–8.
12. Barrett JMG, Clark DE, Hench LL. US Patent 4189325; 1980.
13. Wu J, Cannon WR, Panzera C. US Patent 4515634; 1985.
14. Massiot D, Fayon F, Capron M, King I, Le Calvé S, Alonso B, et al. Modelling one- and two-dimensional solid-state NMR spectra. *Magn Reson Chem* 2002;**40**:70–6.
15. Morimoto S. Effect of K_2O on crystallization of Li_2O–SiO_2 glass. *J Ceram Soc Jpn* 2006;**114**:195–8.
16. James PF. Liquid-phase separation in glass-forming systems. *J Mater Sci* 1975;**10**:1802–25.
17. Shelby JE. *Introduction to glass science and technology*. Cambridge: The Royal Society of Chemistry; 1997.
18. Martin JW. *Concise encyclopedia of the structure of materials*. Amsterdam: Elsevier; 2007.
19. Schneider J, Mastelaro VR, Panepucci H, Zanotto ED. ^{29}Si MAS-NMR studies of Q^n structural units in metasilicate glasses and their nucleating ability. *J Non-Cryst Solids* 2000;**273**:8–18.
20. Schramm CM, de Jong BHWS, Parzialet VE. ^{29}Si magic angle spinning NMR study on local silicon environments in amorphous and crystalline lithium silicates. *J Am Ceram Soc* 1984;**106**:4396–402.
21. de Oliveira APN, Alarcon OE, Manfredini T, Pellacani GC, Siligardi C. Crystallisation kinetics of a $2.3Li_2O{\cdot}1.1ZrO_2{\cdot}6.6SiO_2$ glass. *Phys Chem Glasses* 2000;**41**:100–3.
22. Hammetter WF, Loehman RE. Crystallization kinetics of a complex lithium silicate glass-ceramic. *J Am Ceram Soc* 1987;**70**:577–82.
23. Scholze H. *Glass: nature, structure and properties*. New York/Berlin/Heidelberg: Springer-Verlag GmbH & Co. KG; 1991.
24. Bischoff C, Eckert H, Apel E, Rheinberger VM, Holand W. Phase evolution in lithium disilicate glass-ceramics based on non-stoichiometric compositions of a multi-component system: structural studies by ^{29}Si single and double resonance solid state NMR. *Phys Chem Chem Phys* 2011;**13**:4540–51.